


# Didymin Ameliorates Liver Fibrosis by Alleviating Endoplasmic Reticulum Stress and Glycerophospholipid Metabolism: Based on Transcriptomics and Metabolomics

Yan Li<sup>1,\*</sup>, Cuiyu Li<sup>1,\*</sup>, Yuhua Xiong<sup>1</sup>, Bin Fang<sup>1</sup>, Xing Lin<sup>1</sup>, Quanfang Huang<sup>2</sup>

<sup>1</sup>Life Sciences Institute, Guangxi Medical University, Nanning, Guangxi, 530021, People's Republic of China; <sup>2</sup>The Pharmaceutical Department, Guangxi University of Chinese Medicine First Affiliated Hospital, Nanning, Guangxi, 530023, People's Republic of China

\*These authors contributed equally to this work

Correspondence: Xing Lin, Guangxi Medical University Life Sciences Institute, Nanning, Guangxi, 530021, People's Republic of China, Email [gluck4668@sina.com](mailto:gluck4668@sina.com); Quanfang Huang, The Pharmaceutical Department, Guangxi University of Chinese Medicine First Affiliated Hospital, Nanning, 530023, People's Republic of China, Email [g723m6@sina.com](mailto:g723m6@sina.com)

**Introduction:** *Origanum vulgare* L. is a traditional Chinese herb, having a strong hepatoprotective effect. In our previous experiments, we have isolated an ingredient from this herb and identified it as didymin. This study aimed to investigate the effects and underlying mechanisms of didymin on liver injury and fibrosis, elucidating whether it was the pharmacodynamic material basis of *Origanum vulgare* L.

**Methods:** Mice were injected with CCl<sub>4</sub> for 10 weeks to induce liver fibrosis, followed by didymin treatment for 6 weeks. Then, biochemical analysis and histopathological examinations were conducted to evaluate the therapeutic effects of didymin in alleviating fibrosis. Next, the possible mechanisms of didymin were predicted by transcriptomics and then verified by the multiple relevant examinations.

**Results:** The pharmacodynamic experiments indicated that didymin significantly attenuated CCl<sub>4</sub>-induced hepatic injury and fibrogenesis, as evidenced by the ameliorative pathological tissue, low transaminase activity, and decreased collagen accumulation. Interestingly, the transcriptome analysis predicted that the potential targets were likely to be endoplasmic reticulum stress (ERS), inflammation, apoptosis, and metabolic pathways. And the predictions were then verified by the following examinations: (1) didymin significantly inhibited ERS by regulating the ATF6, IRE1 $\alpha$ , and PERK pathways; (2) didymin markedly alleviated hepatocyte apoptosis by restoring the expression of Bcl-2 and caspase families, as well as the mitochondrial dysfunction; (3) didymin significantly decreased the production of the pro-inflammatory cytokines (IL-1 $\beta$  and IL-6); (4) didymin inhibited the glycerophospholipid metabolism pathway by decreasing the synthesis of phosphatidylethanolamines and phosphatidylcholines.

**Conclusion:** Our findings demonstrate that didymin can ameliorate liver fibrosis, which is mainly attributed to the inhibition of ERS, inflammation, and glycerophospholipid metabolism.

**Keywords:** didymin, transcriptomics, metabolomics, liver fibrosis, endoplasmic reticulum stress, ERS

## Introduction

Liver fibrosis, caused by various risk factors (such as viral infections, alcoholism, and toxins), is a wound-healing response to chronic liver damages, which can lead to cirrhosis and liver cancer without valid interventions.<sup>1</sup> The pathogenesis of liver fibrosis is complex, and endoplasmic reticulum stress (ERS) has been confirmed to be involved in the process. ERS, an essential compensatory mechanism in the liver, can be activated by various physiological or pathological factors, such as intracellular energy levels, oxidative status, and calcium ion concentrations.<sup>2-4</sup> Mounting evidence indicates that ERS is relevant to the development and progression of fibrotic diseases.<sup>5</sup> For liver fibrosis, it is

assumed that ERS has two opposing effects, including adaptation and apoptosis. Although ERS serves a protective role that allows cells to deal with the noxious stimuli, persistent and immense ERS contributes to cell apoptosis.<sup>6</sup> Apoptotic hepatocytes can repeatedly stimulate hepatic stellate cells and immune cells to produce inflammatory factors and cytokines, and then promote liver fibrosis. Thus, reducing ERS might be a promising strategy for reversing the progression of fibrosis.

Metabolic disturbance easily leads to over-production of lipids and lipotoxicity, destroying cytomembrane integrity and sequentially exacerbating hepatic injury.<sup>7</sup> Lipids are the structural building blocks and energy stores, as well as the key molecules in cell signaling, maintenance of homeostasis, and inflammatory and immune response.<sup>8</sup> Glycerophospholipids (GPs), one kind of lipid, have been reported to play an important role in liver fibrosis. The liver as the main metabolic organ is most directly impaired by the disturbed glycerophospholipid metabolism, leading to steatohepatitis and metabolic syndrome, and these changes would increase the risk of developing liver fibrosis.<sup>9</sup> So, seeking an effective way to restore the disorder of lipid metabolism might provide a potential strategy for the treatments of liver fibrosis.

Traditional Chinese Medicine (TCM) has been used to treat chronic diseases for a long time due to its multi-components, multi-targets, and multi-pharmacological effects.<sup>10</sup> *Origanum vulgare* L. is a perennial and herbaceous plant, belonging to the *Lamiaceae* family widespread across China, which has been confirmed to have a strong hepatoprotective effect on carbon tetrachloride-induced hepatotoxicity.<sup>11</sup> In our previous studies, we have successfully isolated a flavone glycoside from this traditional Chinese herb and identified it as didymin. Moreover, we found that it could remarkably alleviate fatty liver mainly by inhibiting oxidative stress and inflammation.<sup>12</sup> To comprehensively understand its therapeutic effects on various liver diseases and develop it as a promising agent for the treatment of liver injury, multiple experimental models of liver injury need to be performed. Transcriptomics and metabolomics belong to the ‘omics’ technologies, which can provide insights into the complex pathogenesis and potential targets of diseases as a whole.<sup>13</sup> Therefore, this study focused on the hepatoprotective effects and underlying mechanisms of didymin on carbon tetrachloride (CCl<sub>4</sub>)-induced liver injury and fibrosis using transcriptomic and metabolomic technology, trying to provide the theoretical evidence for the application of didymin on liver fibrosis.

## Methods

### Animal and Treatment

Male C57BL/6J mice (SPF, 20 ± 2 g) were obtained from the Laboratory Animal Center of Guangxi Medical University (Guangxi, China), and housed in an environmentally controlled condition (temperature 18–22 °C, humidity 60–70%, and natural circadian rhythm and light). This experiment was approved by the Institutional Animal Care and Use Committee, Guangxi Medical University. All the procedures conformed to the National Institute of Health Guidelines on the Use of Laboratory Animals.

As shown in Figure 1, liver fibrosis was induced as previously described.<sup>14</sup> In brief, mice were randomized into 6 groups (n=12) after 1 week of acclimation: the normal control group, model group, 4-Phenylbutyric acid (4PBA) group (400 mg/kg 4-PBA), and didymin-treated groups (2, 1, or 0.5 mg/kg didymin). Except for the normal control group, the mice in the other groups were intraperitoneally injected with 0.5mL/100g CCl<sub>4</sub> (20% v/v, in corn oil) 3 times a week for 10 weeks to induce liver fibrosis,<sup>14</sup> followed by intragastrical administration with 4PBA (a classic ERS inhibitor) or didymin for 6 weeks.<sup>15</sup> The animals in the normal control group were given an equal amount of saline. At the end of the

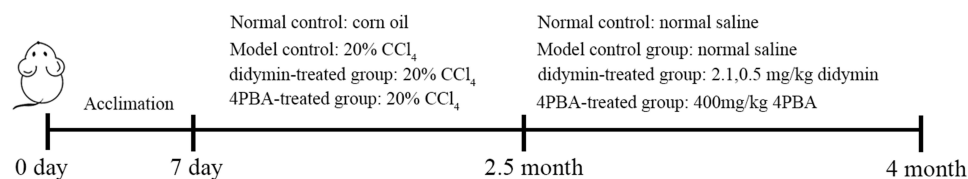


**Figure 1** The experiment schedule.

treatment, all animals were anesthetized by 3% sodium pentobarbital at a dose of 0.1 mL/100 g body weight;<sup>16</sup> the liver tissues and serums were harvested for experiments.

## Serum Analysis

Alanine aminotransferase (ALT), aspartate aminotransferase (AST), and albumin (ALB) in serum specimens were tested with an automatic biochemistry analyzer (Hitachi, Ltd., Kokubunji, Tokyo, Japan).

## Pathological Examination

Hepatic tissues were fixed in 4% paraformaldehyde for 48 hours. Then, liver tissues were embedded by paraffin wax and cut into 4- $\mu$ m slices. These tissue slices were stained with hematoxylin-eosin (H&E) staining, Masson staining and Sirius staining according to standard procedures.

## Terminal Deoxynucleotidyl Transferase-Mediated Nick End Labeling (TUNEL) Assay

TUNEL staining was performed following the manufacturer's instruction using the commercial kit (Beyotime Biotechnology, Nanjing, China). TUNEL-positive cells in the tissue slices with dark brown nuclei mean apoptosis.

## Assessments for Inflammation and Oxidative Stress

The contents of transforming growth factor- $\beta$  (TGF- $\beta$ ), reactive oxygen species (ROS), interleukin-1 $\beta$  (IL-1 $\beta$ ), and interleukin-6 (IL-6) in liver tissue were determined using the ELISA kits (Wuhan Elabscience Biotechnology Co., Ltd., Wuhan, China) according to the assay procedure.

Liver tissues were homogenized in PBS buffer and centrifuged to obtain the supernates. Then the contents of nitric oxide (NO), inducible nitric oxide synthase (iNOS), superoxide dismutase (SOD), glutathione (GSH), and catalase (CAT) were spectrophotometrically detected by commercial kits, and calculated using the protein concentrations as the standard, which were measured by BCA kit.

## Transcriptome Sequencing

RNA sequences analysis was performed by Shanghai Jiayin Biotechnology Co., Ltd as previously described.<sup>17</sup> In brief, 0.1 g liver tissue samples were homogenized with Trizol<sup>TM</sup> reagent (Thermo Fisher Scientific, Lot.15596018) to extract total RNA. The RNA sequencing (RNA-Seq) library was constructed with NEBNext Ultra<sup>TM</sup> RNA Library Prep Kit (NEB E7490). After being enriched with AmpureXP beads, the RNA was fragmented into 200–300 bp pieces by fragmentation buffer. Next, RNA was used as a template and reversed into cDNA by using random hexamer primers (Illumina) and a SuperScript double-stranded cDNA synthesis kit (Invitrogen, CA). After being purified, cDNA was barcoded with multiplex adapters and amplified a cDNA library (Illumina, Inc.; cat. no. PE-300-2001). The total library was quantified by TBS380 and sequenced with the Illumina Novaseq 6000 PE150 (Illumina). The raw sequencing data were filtered by Cutadapt, and the differentially expressed genes (DEGs) with a value of  $|\log_2(\text{fold change})| > 1$  and  $p\text{-values} < 0.05$  were screened out for further analysis.

## Western Blot

The whole liver tissue lysates were prepared as previously described.<sup>18</sup> Briefly, total protein was obtained from liver tissues with RIPA lysis buffer (Solarbio, Beijing, China) containing with 1% phosphatase inhibitor cocktail (CoWin Biosciences, Beijing, China) and 1% protease inhibitor cocktail (Solarbio, Beijing, China). The protein concentration was quantitated with a bicinchoninic acid protein assay kit (Beyotime Institute of Biotechnology) before incubation with loading buffer at 100 °C for 10 minutes. After that, the proteins were separated with the SDS-PAGE gels (EpiZyme, Shanghai, China) and then transferred onto a PVDF membrane (Millipore, Billerica, MA, USA). The membranes were incubated with corresponding primary antibodies overnight at 4 °C: Collagen I (proteintech, 14695-1-AP), Collagen III (proteintech, 22734-1-AP),  $\alpha$ -SMA (proteintech, 14395-1-AP), GRP78 (proteintech, 11587-1-AP), PERK (Cell Signaling Technology (CST), 5683), p-PERK (CST, 3179), IRE1 $\alpha$  (CST, 3294), p-IRE1 $\alpha$  (Signalway Antibody, 13013), IRE1 $\alpha$  (CST, 3294), eIF2 $\alpha$  (proteintech, 11170-1-AP), p-eIF2 $\alpha$  (CST, 3398), ATF6 (proteintech, 24169-1-AP), CHOP

(proteintech, 15204-1-AP), JNK (proteintech, 24164-1-AP), p-JNK (proteintech, 80024-1-RR), Bax (proteintech, 60267-1-Ig), Bcl2 (proteintech, 12789-1-AP), Caspase 3/ Cleaved Caspase 3 (proteintech, 66470-2-Ig), Caspase 9/ Cleaved Caspase 9 (proteintech, 66169-1-Ig), Cytochrome C (proteintech, 10993-1-AP), followed by incubation with fluorescence-labeled rabbit/mouse anti-goat IgG (Invitrogen, USA) under agitation for 1 h at room temperature in the dark. Finally, the band was detected by Image Studio Lite software (LI-COR Biosciences, NE, USA) and quantified through the Image J software.

## RT-PCR

Total RNA was extracted from liver tissues using TRIzol™ reagent (Corning Life Sciences Co., Ltd., Jiangsu, China) and reversely transcribed to cDNA using the Primescript™ RT Master Mix Kit (Takara; RR036A). Transcript levels were measured in duplicate by qRT-PCR (Bio-Rad) using SYBR Green I (Takara Biotechnology, Dalian, China). Expression levels were normalized to  $\beta$ -actin. Primer sequences are listed in Table 1.

## Metabolomics Analysis

Liver samples (100 mg) were homogenized with 800  $\mu$ L prechilled methanol; after vortex mixing for 1 min and sequentially standing still for 15 min in an ice-water bath, the samples were centrifuged at 4°C, 15,000 rpm for 10 min to obtain a 400  $\mu$ L supernatant.<sup>19</sup> The supernatant was filtered with a syringe microfilter (0.22  $\mu$ m). The quality control (QC) sample was prepared by pooling 10  $\mu$ L aliquots from each of the processed supernatants of all samples.

Next, the supernatants were analyzed by Ultra-performance liquid chromatography equipped with quadrupole time-of-flight mass spectrometry (UPLC-Xevo G2-XS QToF, Waters, USA). Briefly, chromatographic separation was performed by using Acquity UPLC® BEH C18 column (50×2.1 mm, 1.7  $\mu$ m, Waters Crop.) at a flow rate of 0.3 mL/min. The mobile phases consisted of water with 0.1% formic acid (A) and acetonitrile with 0.1% formic acid (B), and the gradient elution system was set as follow: 0 min, 5% B; 1 min, 20% B; 2.5 min, 40% B; 9min, 90% B; 10min, 100% B; 12.5min, 100% B and 14min, 5% B. In each run, the injection volume was 2  $\mu$ L and the time was held at 15min. The column temperature was maintained at 45 °C while the autosampler tray temperature was at 4°C. Then, mass spectrometry was carried out in the positive ion mode. The mass range was from 50 to 1200 Da. Source and desolvation temperatures were set at 150°C and 350°C, respectively. The capillary voltage and cone voltage were 250 kV and 40 V, respectively. Nitrogen was used as both cone gas (50 L/h) and desolvation gas (800 L/h). Argon was set as collision gas. The data were analyzed with MassLynx V4.1, Progenesis QI V2.4, and EZinfo V3.0 (Waters Inc.).

## Statistical Analysis

The statistical analysis was implemented using SPSS (version 17.0, USA). Data were expressed as mean  $\pm$  standard deviation. The inter-group comparison was analyzed by one-way analysis of variance (ANOVA). Differences at  $p < 0.05$  were considered statistically significant.

## Results

### Didymin Might Target the Liver Tissue

To observe whether didymin could target the liver, the metabolism of didymin was detected by UPLC-Qtof-MS with UNIFI Portal Software. As shown in Figure 2, the parent and fragment ions of didymin were discovered in the liver

**Table 1** The Sequences of Primers Used for Real-Time Quantitative PCR

Genes	Forward Primer (5'-3')	Reverse Primer (5'-3')
<i>GRP78</i>	TGTGTGTGAGACCAGAACCG	AACACACCGACGCAGGAATA
<i>Chop</i>	CCTGAGGAGAGAGTGTCCAG	GACACCGTCTCCAAGGTGAA
<i><math>\beta</math>-actin</i>	GTGCTATGTTGCTCTAGACTTCG	ATGCCACAGGATTCCATACC

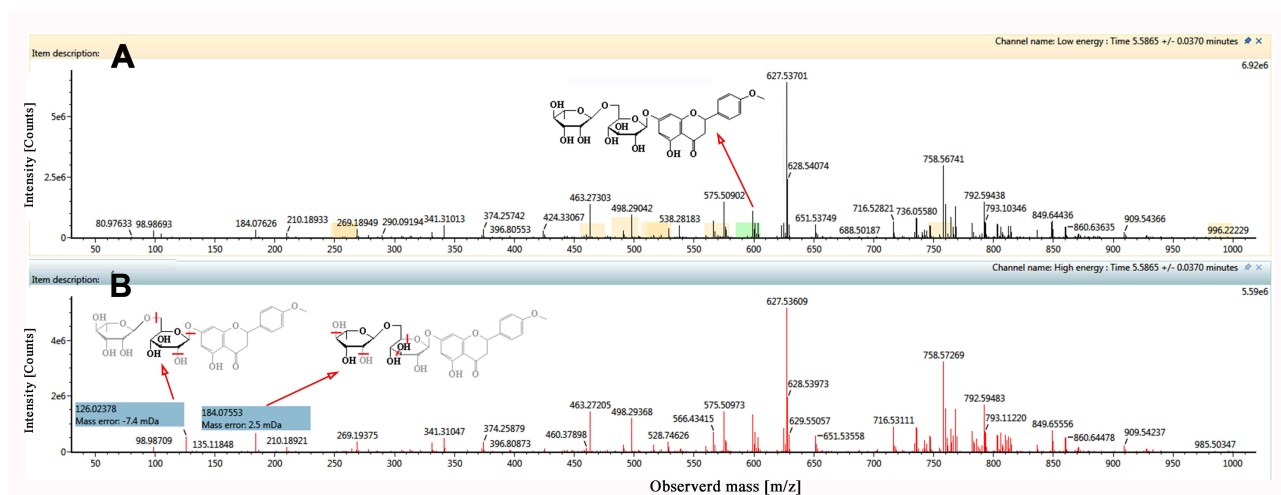


**Figure 2** Didymin was identified by UNIFI Portal in the liver tissue. **(A)** The parent ion of didymin; the pale green indicates the peak of didymin; **(B)** the fragment ions of didymin; the pale blue indicates the peaks of the fragments of didymin.

tissue, suggesting that didymin could be absorbed and degraded by the liver. The liver likely was the target organ of didymin.

## Didymin Attenuated Liver Injury in Mice

As shown in [Figure 3A](#), the livers of mice treated with  $\text{CCl}_4$  exhibited obvious hepatocellular damages: the destroyed hepatic lobules, thickened central venous wall, fibrous hyperplasia, and excessive inflammation infiltration, which was consistent with the previous report (the raw data of HE staining can be found in [Figure S1](#)).<sup>20</sup> However, compared with the model group, didymin administration effectively attenuated the  $\text{CCl}_4$ -induced liver injury, especially in decreasing the degrees of fibrous septa and inflammatory cells infiltration. Furthermore, the serum AST and ALT levels, the biomarkers of liver injury, were significantly increased in the  $\text{CCl}_4$  group, while were alleviated in the didymin group. ([Figure 3B and C](#)); ALB showed an opposite trend: a remarkable decrease in the  $\text{CCl}_4$  group and an increase in the didymin group ([Figure 3D](#)). These results suggested that didymin could alleviate liver injury in a dose dependent manner. After careful statistical comparison, a significant difference was found between low-dose group (0.5 mg/kg) and the other two groups (2 and 1 mg/kg), indicating didymin in 2 mg/kg and 1 mg/kg has a better treatment effect.

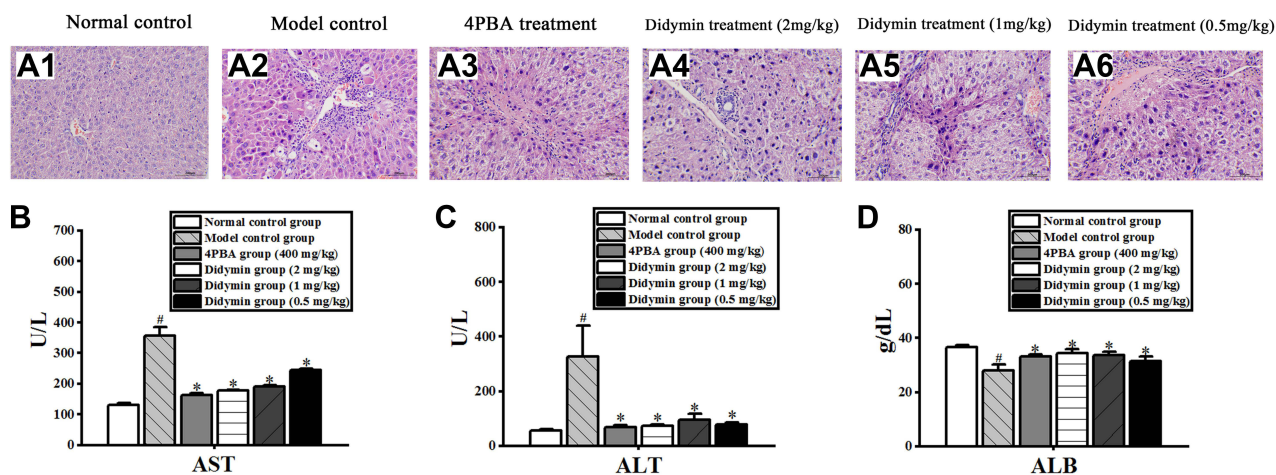


**Figure 3** Didymin attenuated liver injury in mice. **(A)** H&E staining was used to observe the histological changes (200 $\times$ ); **(B–D)** Serum AST, ALT, and ALB were determined using an automatic biochemistry analyzer. A1 to A6 represented the normal, model, 4PBA, and didymin groups (2, 1, and 0.5 mg/kg), respectively. <sup>#</sup> $P < 0.05$  VS the normal group and <sup>\*</sup> $P < 0.05$  VS the  $\text{CCl}_4$  model group.

## Didymin Alleviated Collagen Accumulation

Sirius red and Masson staining were used to assess the extent of collagen deposition. As shown in Figure 4A and B, amounts of collagen were observed around the central vein and in the confluent area of the liver in the CCl<sub>4</sub> group, whereas treatment with didymin markedly reduced collagen deposition (the raw data of Sirius and Masson staining can be found in Figures S2 and S3). CCl<sub>4</sub> exposure caused a significant increase in the levels of collagen-I and -III (Col-I and Col-III), as well as  $\alpha$ -SMA and TGF- $\beta$  (an important profibrotic cytokine in hepatic fibrosis), while didymin or 4PBA markedly reversed these abnormal changes (Figure 4C–F). A significant difference was found in the expressions of Col-I and Col-III in the three dose groups. These results indicated that didymin treatment could reduce hepatic fibrogenesis in a dose dependent manner (the raw data of collagen related proteins were shown in Figure S4).

## Didymin Induced Transcriptomic Alterations

Transcriptomics can provide the global change of genes, which is beneficial for exposing the complex pathological mechanism. In the current study, transcriptomic analysis was carried out to predict the potential targets or the relevant regulatory pathways. As shown in Figure 5A, the Principal Component Analysis (PCA) diagram revealed a significant dispersion among the normal, model, and the didymin groups, suggesting the different genes among them. Moreover, the heatmap plot showed that a part of genes in the normal, model and didymin group showed a trend: down, up, and down; the other part showed an opposite trend (Figure 5B). The volcano plot showed that CCl<sub>4</sub> significantly up-regulated 1188 genes and down-regulated 1190 genes compared to the normal control group; after didymin administration, there were 1820 up-regulated and 1134 down-regulated DEGs compared to the model group (Figure 5C).

Next, the DEGs-related biological function and pathways were analyzed using the KEGG database. GO analysis showed that these DEGs might involve in the biological process (BP), cellular component (CC), and molecular function (MF) (Figure 5D). For the up-regulated genes, the DEGs could enrich into several pathways, and the metabolic pathways and inflammation were closely associated with liver fibrosis (Figure 5E). On the other hand, the down-regulated genes were mainly enriched into 10 pathways; among them, endoplasmic reticulum stress (ERS) could contribute to

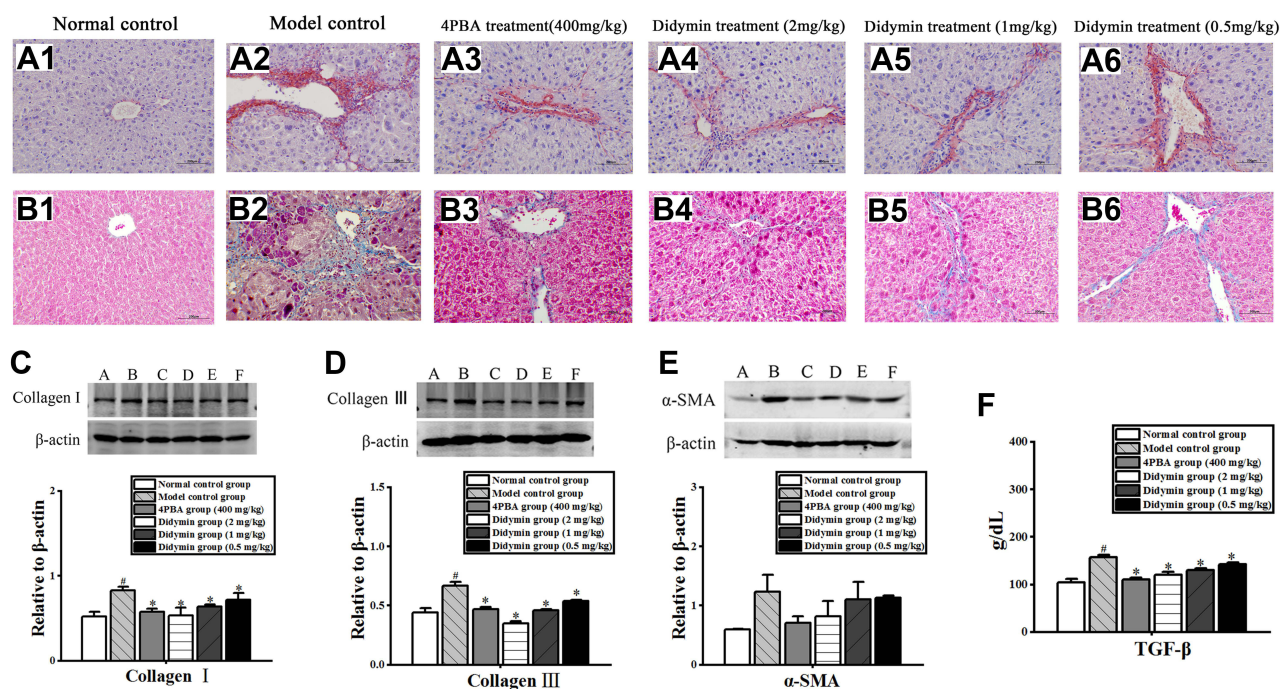


**Figure 4** Didymin alleviated collagen accumulation. (A and B) Sirius staining and Masson staining were used to observe collagen accumulation (200 $\times$ ). A1 to A6 (or B1 to B6) represented the normal, model, 4PBA, and didymin group (2, 1, and 0.5 mg/kg), respectively; (C–E) The protein expression of Col-I, Col-III and  $\alpha$ -SMA was detected by Western blotting; bands 1–6 represented the normal, model, 4PBA, and didymin-treated groups (2, 1, and 0.5 mg/kg), respectively; (F) The content of TGF- $\beta$  was detected by ELISA. #P<0.05 VS the normal group and \*P<0.05 VS the CCl<sub>4</sub> model group.

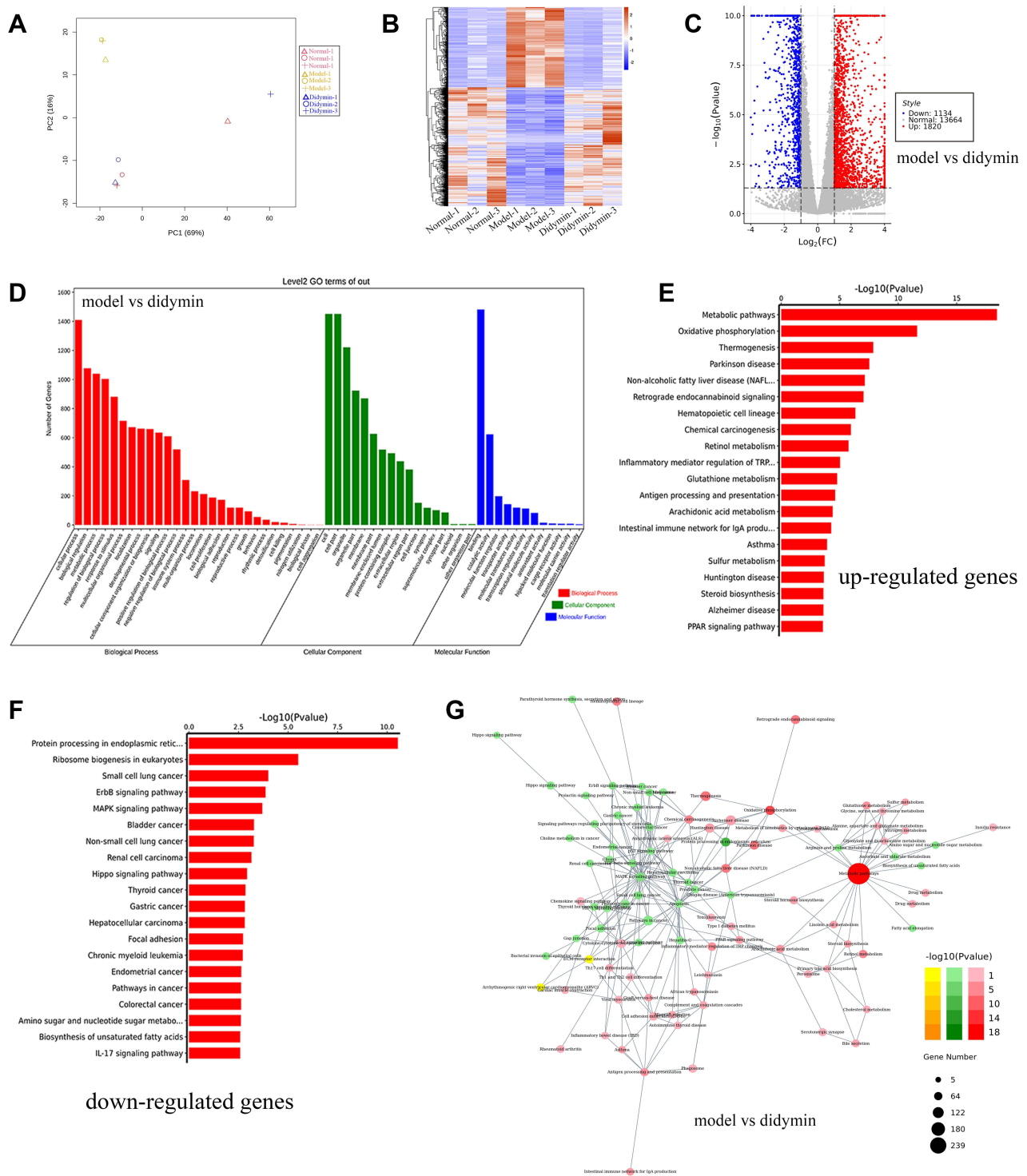


**Figure 5** Didymn induced transcriptomic alterations. **(A)** Principal component analysis (PCA) diagram; **(B)** Heatmap diagram (the red plots mean high gene expression level); **(C)** volcano plot; **(D)** gene ontology (GO) analysis; **(E and F)** KEGG pathway analysis (among up-regulated genes and down-regulated genes); **(G)** network was built based on the relationship between KEGG Pathways.

fibrogenesis (Figure 5F). Furthermore, all these DEGs were mapped into a gene network, and the metabolic pathways got the highest score (Figure 5G). Summarily, the transcriptomic analysis predicted that didymn might target ERS, inflammation, and metabolic pathways. Then, the prediction needs to be verified in the following experiments.

## Didymin Reduced Endoplasmic Reticulum Stress

Since the transcriptome profile suggested that didymin could inhibit the expressions of ERS-related genes, we supposed it might be a crucial way for didymin to alleviate hepatic fibrogenesis. As shown in Figure 6A–F, the protein expressions of GRP78, XBP-1, p-eIF2 $\alpha$ /eIF2 $\alpha$ , p-IRE1 $\alpha$ /IRE1 $\alpha$ , ATF6 and p-PERK/PERK were markedly increased in the model group. However, didymin or 4-PBA significantly decreased the expression of these ERS-related markers. CHOP and p-JNK, which play key roles in ERS-mediated apoptosis, were significantly up-regulated in the mice with CCl<sub>4</sub> exposure, whereas the expressions of CHOP and p-JNK were notably attenuated by didymin administration (Figure 6G and H). Similarly, the RNA expression of GRP78 and CHOP were also attenuated by didymin (Figure 6I and J). Taken together, these results suggested that didymin could reduce ERS by inhibiting the ATF6, IRE1 $\alpha$ , and PERK paths, which verified the prediction of transcriptomic analysis above (the raw data of ERS related proteins were shown in Figure S5).

## Didymin Attenuated Oxidant Stress and Inflammation

To verify whether didymin relieved CCl<sub>4</sub>-induced hepatic fibrosis through inhibiting inflammatory responses, pro-inflammatory cytokines were measured by ELISA kits. As shown in Figure 7A and B, the levels of IL-1 $\beta$  and IL-6 were markedly increased in the CCl<sub>4</sub> group; however, didymin treatment significantly reversed these abnormal changes.

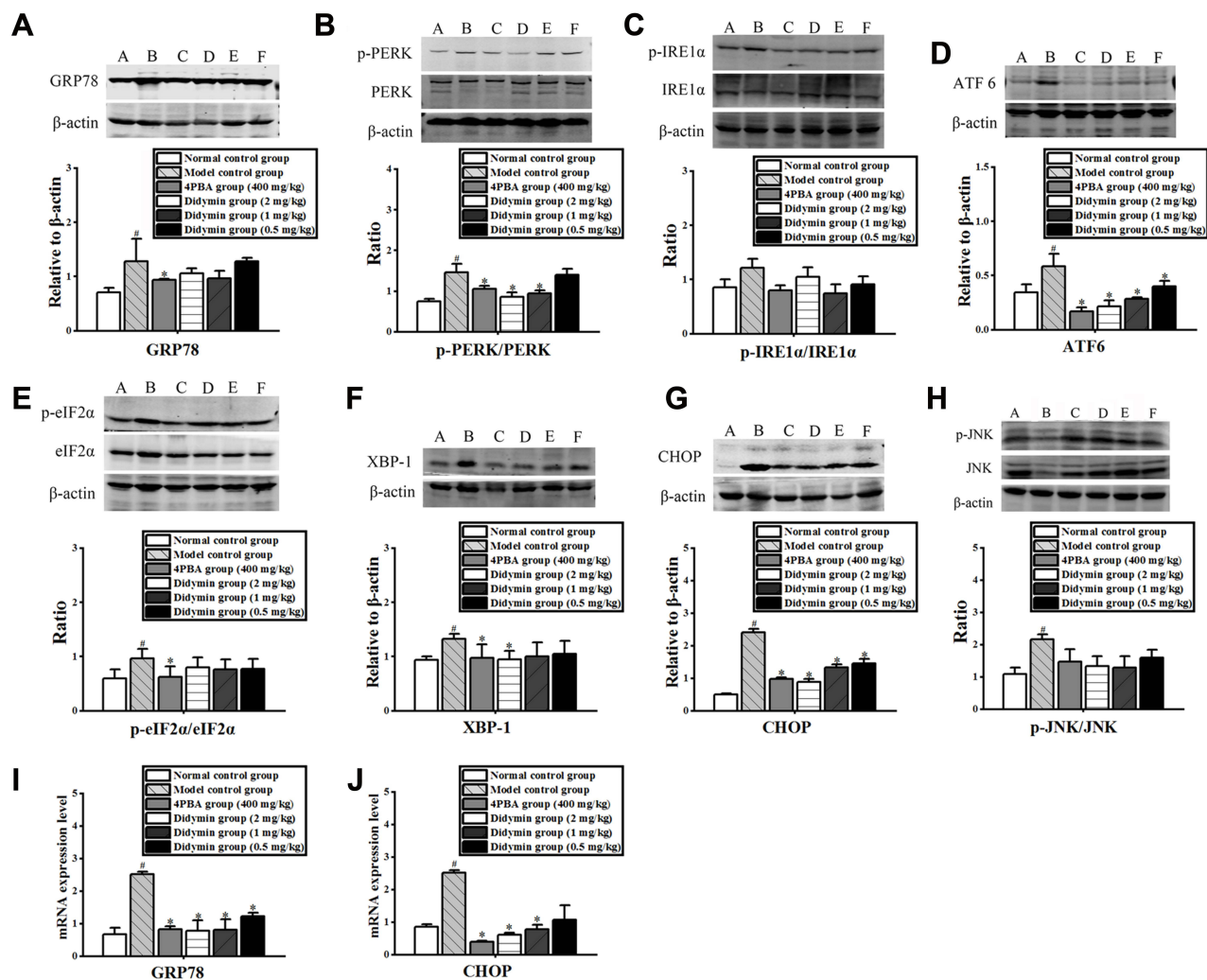


**Figure 6** Didymin reduced ERS by inhibiting the relevant signaling pathways. (A–H) The protein expression of GRP78, PERK, IRE1 $\alpha$ , ATF 6, eIF2 $\alpha$ , XBP-1, CHOP and JNK was detected by Western blotting; bands 1–6 represent the normal group, model control group, 4PBA group, and didymin-treated groups (2, 1 and 0.5mg/kg), respectively; (I and J) The mRNA levels of GRP78 and CHOP were detected by RT-PCR. #P<0.05 VS the normal group and \*P<0.05 VS the CCl<sub>4</sub> model group.



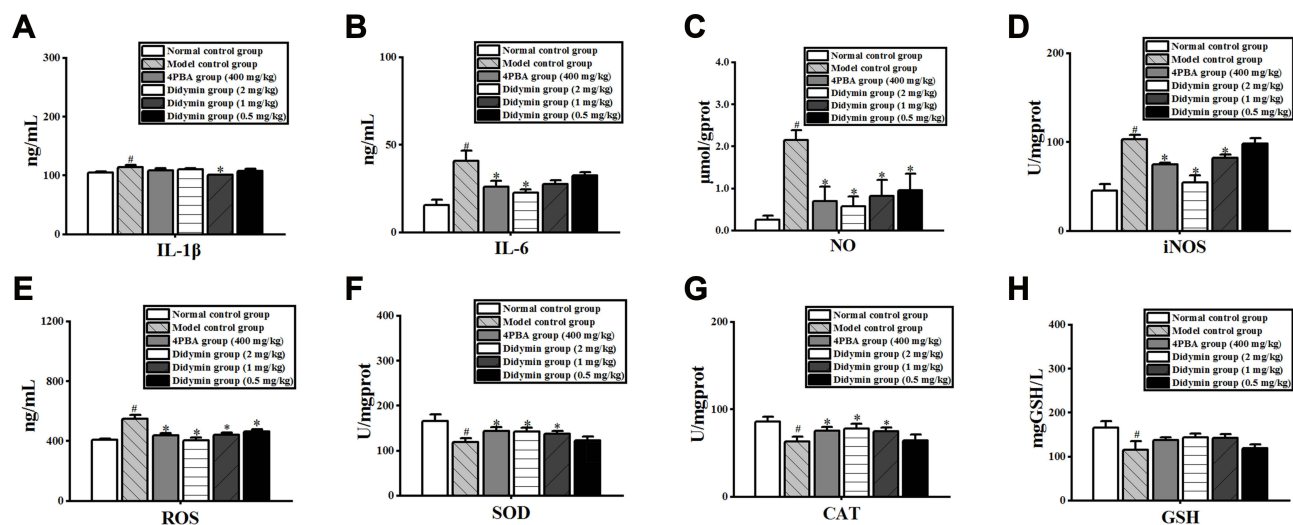


**Figure 7** Didymin alleviated inflammation and oxidant stress. **(A and B)** The contents of IL-1 $\beta$  and IL-6 in the liver were determined with the ELISA kits. **(C and D)** The activity of iNOS and the content of NO in the liver were determined with the commercially-available kits. **(E–H)** The content of ROS and the activities of antioxidant enzymes were determined using the commercially-available kits. # $P < 0.05$  VS the normal group and \* $P < 0.05$  VS the CCl<sub>4</sub> model group.

Besides, iNOS and NO were significantly increased in the model group, which were positively correlated with inflammation (Figure 7C and D); however, they were markedly decreased after didymin administration. We also further assessed the concentration of reactive oxygen species (ROS) and the activity of antioxidant enzymes, which play crucial roles in oxidative stress responses. As shown in Figure 7E to H, ROS was significantly increased and the activity of SOD, CAT, and GSH was markedly decreased in the CCl<sub>4</sub> group. Administration with didymin effectively attenuated the abnormal increase of ROS and enhanced the activity of SOD, CAT, and GSH (the raw data of the oxidant stress and inflammation assays are in Table S1).

## Didymin Alleviated Hepatic Apoptosis

Excessive hepatic apoptosis can cause liver tissue damage. As shown in Figure 8A, TUNEL staining revealed numerous positive apoptotic hepatocytes in the model group and less in the didymin treatment groups (the raw data of TUNEL staining were shown in Figure S6). The further mechanism studies indicated that didymin significantly reduced the ratios of Bax/Bcl-2, cleaved-caspase3/caspase3 and cleaved-caspase 9/caspase 9 (Figure 8B–E). Moreover, didymin treatment markedly protected mitochondria integrity, as evidenced by the decreased release of cytochrome C from mitochondria into the cytoplasm (Figure 8F). The data above indicated that didymin could reduce hepatic apoptosis by regulating the Bcl-2 and caspase families and ameliorating mitochondria injury, which was consistent with the transcriptomic analysis (the raw data of apoptosis related proteins were found in Figure S7).

## Effects of Didymin on Metabolites

Metabolic disorder may cause various liver dysfunctions, which is likely a potential target to intervene in liver diseases. According to the prediction of transcriptomic analysis, a non-target metabolomics approach was performed to verify the effect of didymin on the metabolism profile. As shown in Figure 9, the PCA plot revealed a relatively tight clustering among the QC samples, and the Hotelling's T<sup>2</sup> Range revealed a high correlation coefficient. Moreover, the total ion chromatograms (TICs) showed nearly the same shape. These data suggested that the condition for metabolic analysis was stable and could be used for the following assays.

The PCA diagram revealed a distinct distribution among the normal, model and didymin groups (Figure 10A), which was also confirmed by the Heatmap plot (Figure 10B). Next, the OPLS-DA plot was applied to characterize the separation between two different groups and then to find discrepant compounds via variable importance in the projection (VIP). After selecting with the filtering condition of VIP value  $\geq 1$  and  $p < 0.05$ , there were 219 different metabolites

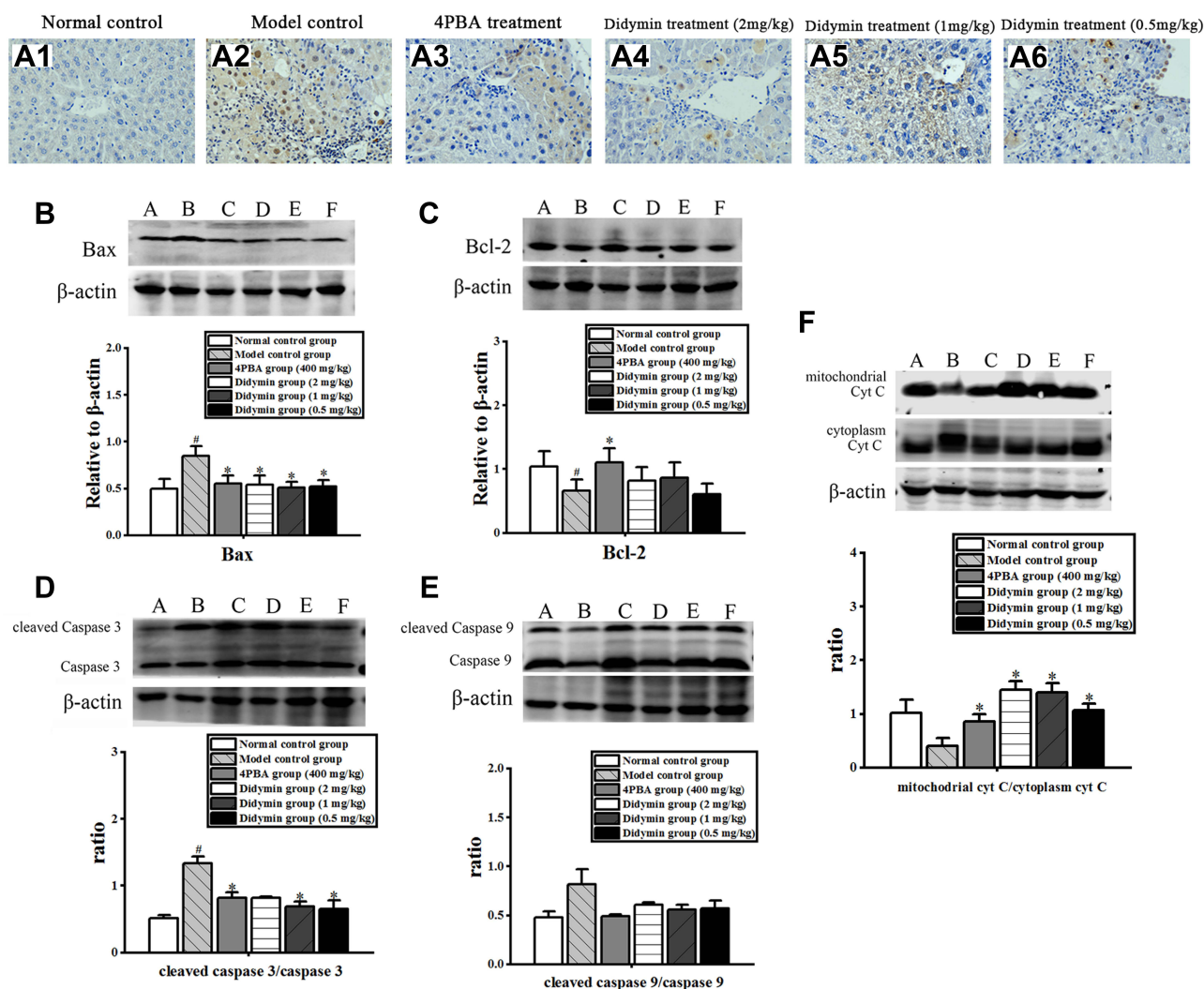


**Figure 8** Didymin reduced hepatic apoptosis. (A) TUNEL staining was used to observe the apoptosis levels (400 $\times$ ), A1 to A6 represented the normal, model, 4PBA, and didymin groups (2, 1, and 0.5 mg/kg), respectively; (B–F) The protein expressions of Bax, Bcl-2, Cyt C, cleaved caspase3/caspase3 and cleaved caspase9/caspase9 were detected by Western blotting; bands 1–6 represent the normal group, model control group, 4PBA group, and didymin-treated groups (2, 1, and 0.5 mg/kg), respectively. <sup>#</sup>P<0.05 VS the normal group and <sup>\*</sup>P<0.05 VS the CCl<sub>4</sub> model group.

between the CCl<sub>4</sub> group and normal group, and 454 between the didymin-treatment group and the model group (Figure 10C–F). Next, the relevant metabolic pathways were analyzed by MetaboAnalyst 5.0 (<https://www.metaboanalyst.ca/MetaboAnalyst/>) and the results suggested that the different metabolites between the didymin-treatment group and the model group were mainly enriched in the glycerophospholipid metabolism pathway (Figure 10G and H). Further investigation revealed that C00157 (phosphatidylethanolamine (PE)) and C00350 (Phosphatidylcholine (PC)) likely were the targets of didymin to regulate glycerophospholipid metabolism.

## Integrative Analysis of the Transcriptomics and Metabolomics

The metabolomic analysis indicated that didymin could affect the glycerophospholipid metabolism pathway. To further understand how didymin regulated this pathway, the integrative analysis of transcriptomics and metabolomics was carried out. As shown in Figure 11A, the integrative analysis predicted that the synthesis of the phosphatidylethanolamine (C00350) and phosphatidylcholine (C00157) might be regulated by the target genes LPCAT1, LPCAT3, LPIN1, PCYT1 $\alpha$ , PCYT2, and DGKZ. Then, further examination indicated that didymin significantly reduced the contents of phosphatidylethanolamine (C00350: PE(16:0/18:2(9Z, 12Z))) and phosphatidylcholine (C00157: LysoPC(P-16:0)), as well as the expressions of the target genes, which confirmed the prediction above (Figure 11B).

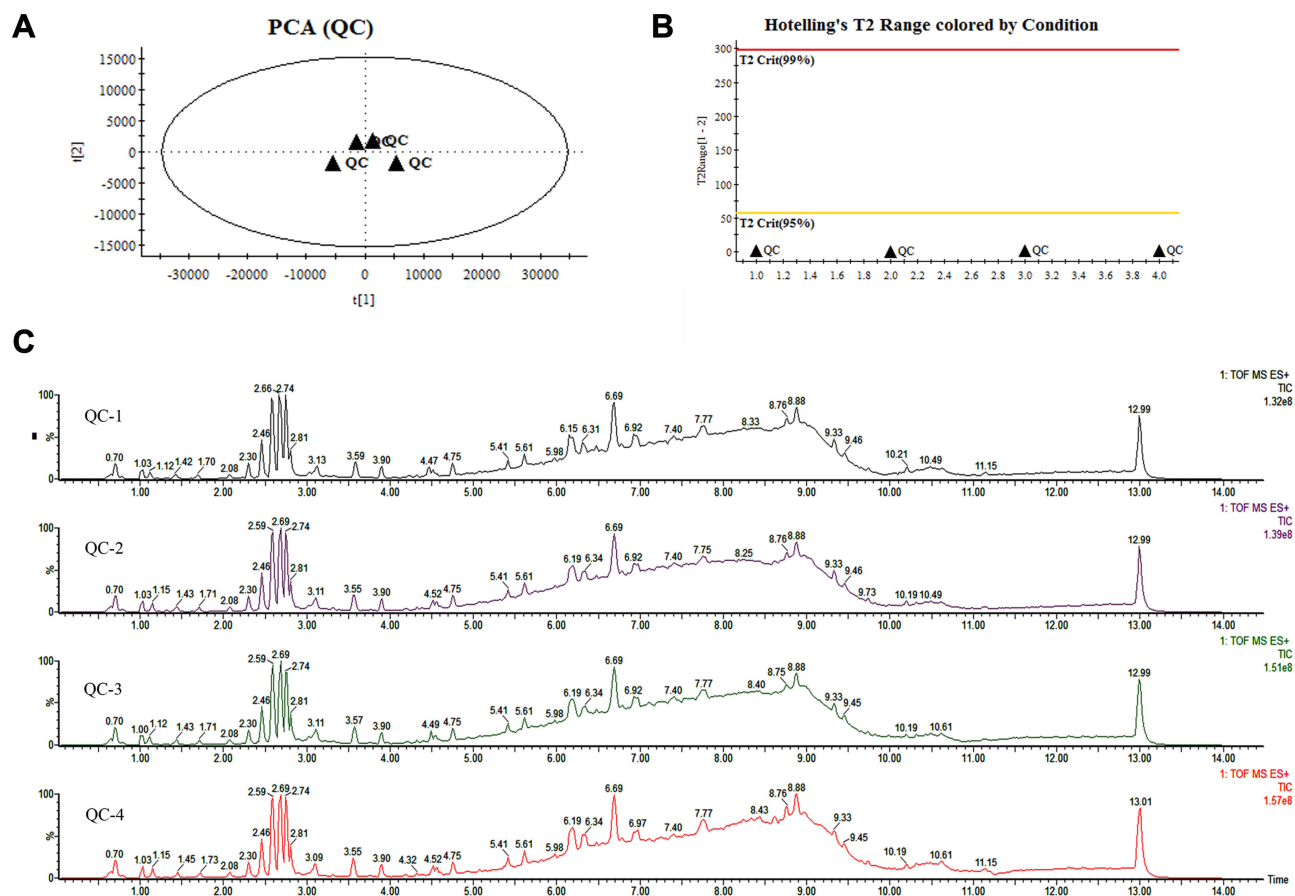
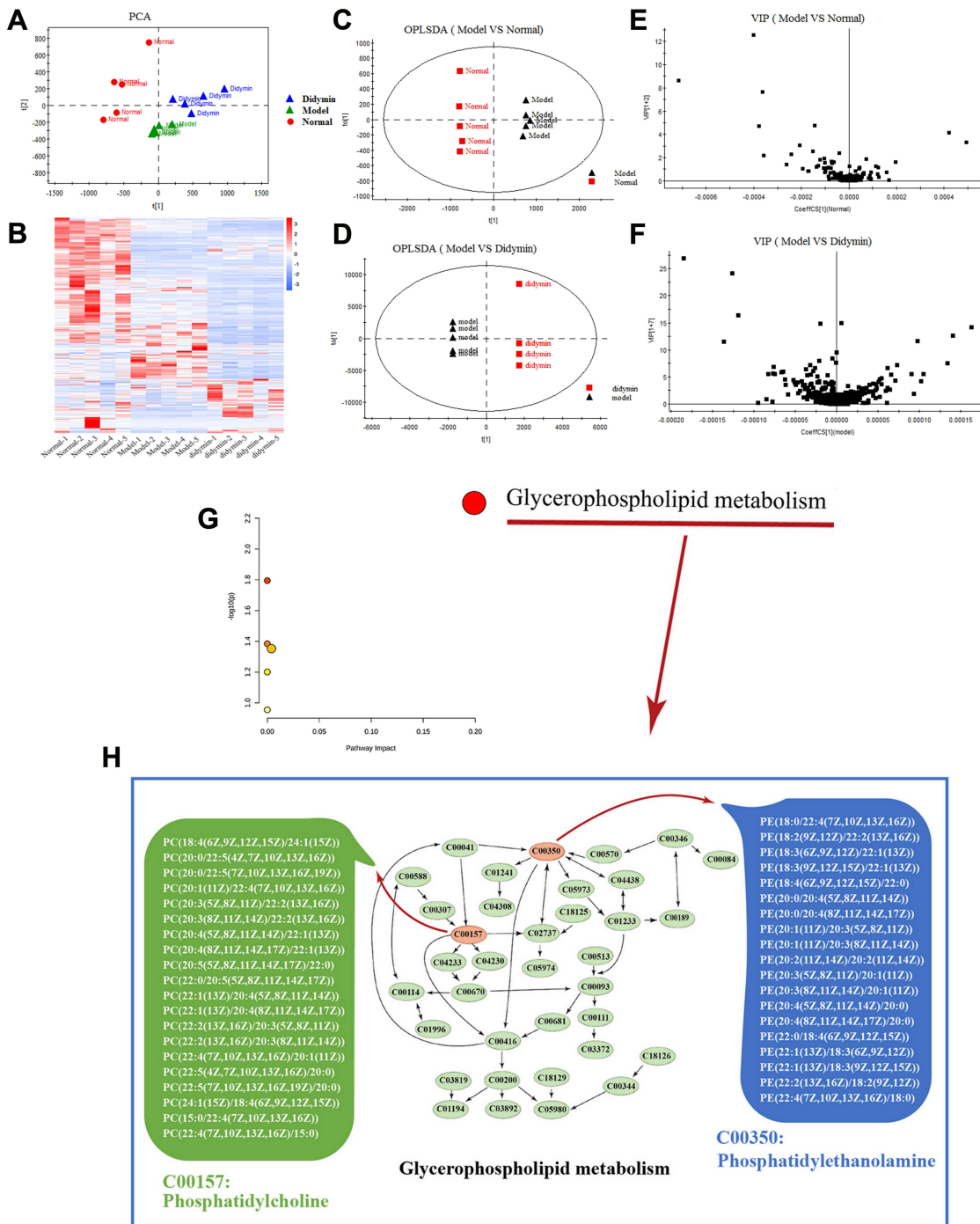


**Figure 9** The quality control (QC) analysis for the metabolomics. **(A)** The principal component analysis (PCA) was used to score the sample. Each point in the plot corresponds to an observation. Observations near each other in the plot mean similar; observations far away from each other mean dissimilar. **(B)** The Hotelling's T2 Range was also used to evaluate the distribution; the plot shows how far away an observation is from the center of the model. **(C)** The total ion chromatogram (TIC) of QC samples.

## Discussion

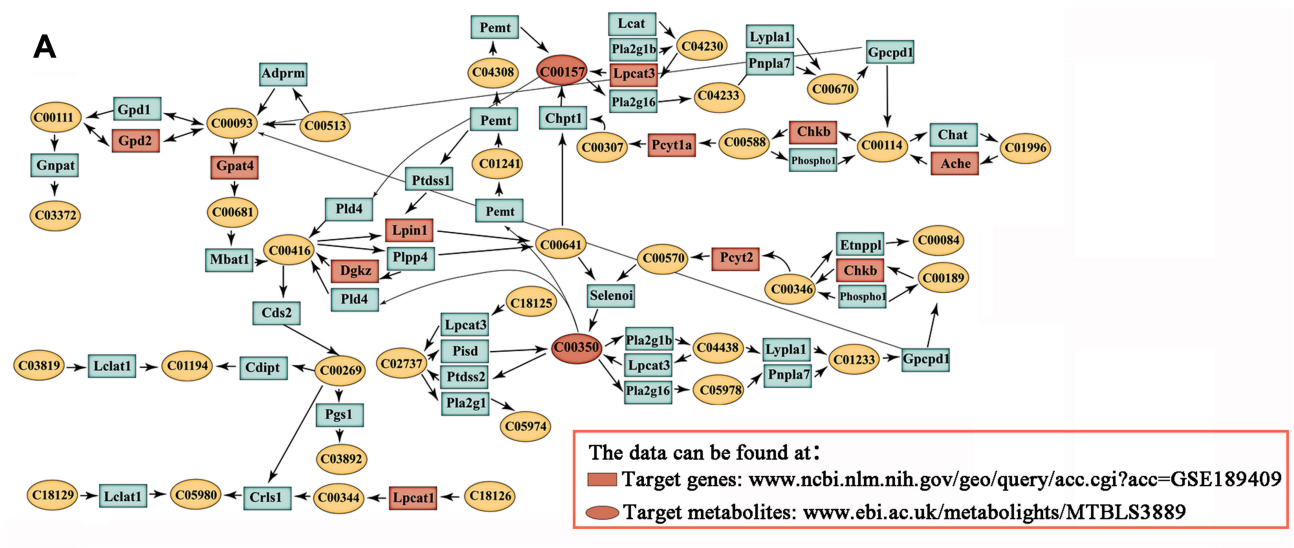
In this study, the liver fibrosis model was induced by  $\text{CCl}_4$ , a quite mature liver fibrosis model. The pathological examination revealed that didymin significantly alleviated  $\text{CCl}_4$ -induced hepatocyte damage, which was confirmed by the improvement of the liver function, as evidenced by the decreased levels of AST and ALT. The main characteristic of liver fibrosis is excessive collagen accumulation, and the activation of hepatic stellate cells (HSCs) plays a key role in fibrogenesis. The current study found that didymin remarkably ameliorated collagen formation, as shown in the Masson staining and Sirius staining, and inhibited the collagen-related markers (Col-I and Col-III) expression; besides, the expression of  $\alpha$ -SMA (an indicator of hepatic stellate cell activation) and TGF- $\beta$  (a cytokine that strongly induces HSC activation) was also inhibited by didymin treatment. These results indicated that didymin could alleviate liver fibrosis by reducing collagen accumulation and inhibiting HSCs activation. Interestingly, the UPLC-Qtof-MS analysis showed that didymin could be found in the liver tissue instead of the blood, suggesting that didymin may be developed as a targeting medicine for treating liver fibrosis.

The pathogenesis of liver fibrosis is complex and may involve various risk factors. Transcriptomics can reflect the global changes of genes and might provide insight into the complex pathomechanism. In the current study, transcriptomic analysis was performed to observe the effects of didymin on the abnormally changed genes induced by  $\text{CCl}_4$ , predicting the potential targets or relevant paths as a whole. The analysis indicated that there were 2954 DEGs between the didymin and model groups, which were mainly enriched into endoplasmic reticulum stress (ERS), liver metabolism and



This pathway was analyzed and cited from MetaboAnalyst 5.0 (<https://www.metaboanalyst.ca/MetaboAnalyst/>)  
 The data were published at [www.ebi.ac.uk/metabolights/MTBLS3889](http://www.ebi.ac.uk/metabolights/MTBLS3889)

**Figure 10** Effects of Didymin on metabolites. **(A)** The PCA was analyzed by the Omicshare database (<https://www.omicshare.com/tools/>). **(B)** The Heatmap was analyzed by the Omicshare database (<https://www.omicshare.com/tools/>); the red plots represent the high abundance of metabolite, and the blue plots mean low abundance. **(C)** The OPLS-DA of the model vs normal. **(E)** The VIP diagram of the model vs normal. **(D)** The OPLS-DA of the didymin vs model. **(F)** The VIP diagram of the didymin vs model. **(G)** The metabolic pathways regulated by didymin were analyzed by MetaboAnalyst 5.0. **(H)** The Glycerophospholipid metabolism pathway; C00157: Phosphatidylcholine; C00350: Phosphatidylethanolamine.



### B The Glycerophospholipid metabolism pathway-related metabolites and genes

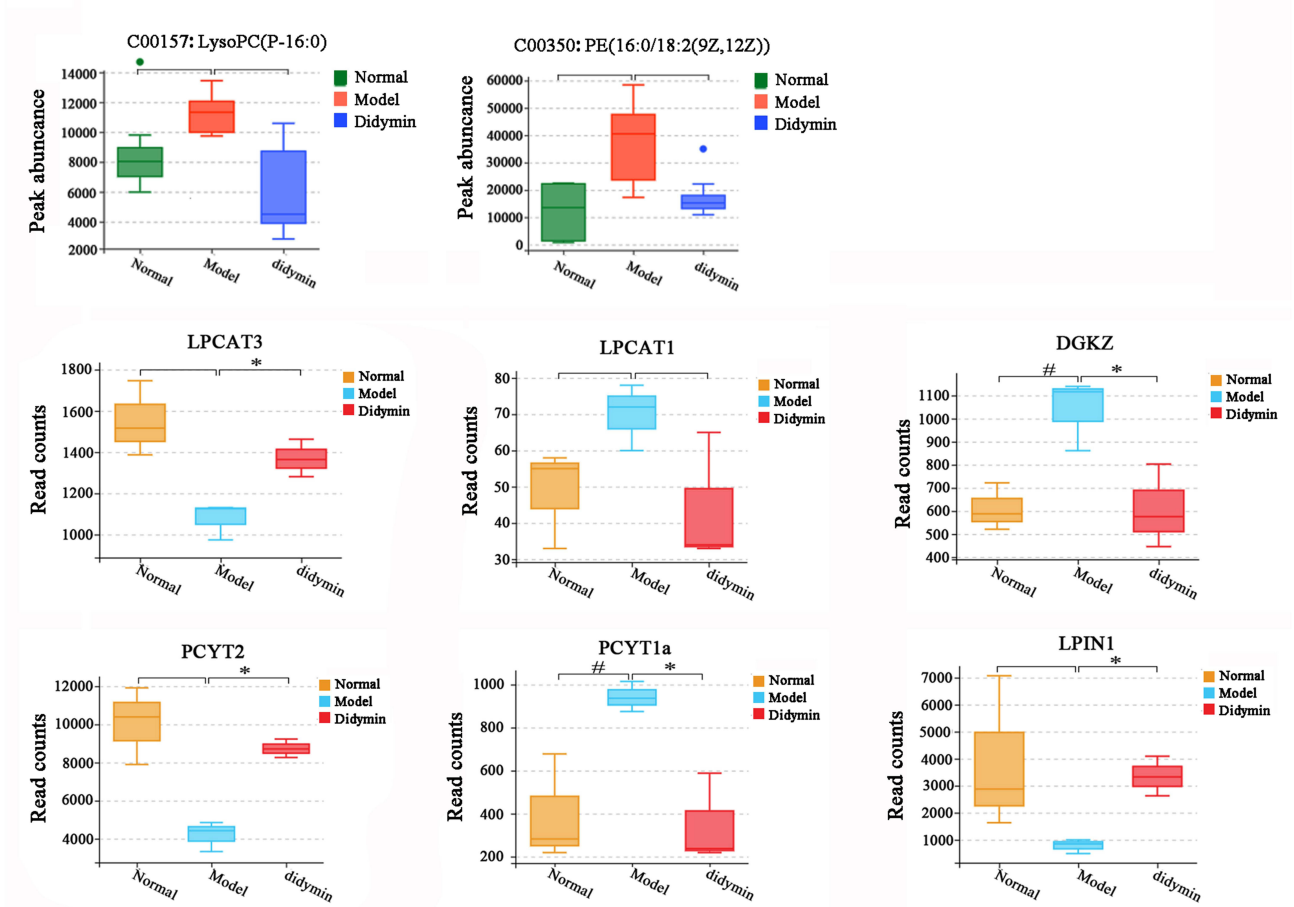


**Figure 11** Integrative analysis of transcriptomics and metabolomics. (A) The integrated relationship between metabolites and genes in Glycerophospholipid metabolism pathway; (B) the contents of Glycerophospholipid metabolism pathway-related metabolites and the expression levels of the target genes. #P<0.05 VS the normal group and \*P<0.05 VS the CCl<sub>4</sub> model group.

inflammation, suggesting they might be involved in the regulatory effects of didymin in ameliorating liver injury and fibrosis. Of course, these predictions need to be verified by the following experiments.

Based on the prediction of transcriptomic analysis, ERS was considered one of the vital mechanisms of didymin against liver fibrosis. In the normal state, ERS is initially protective, aiming to reduce misfolded proteins, restore ER homeostasis and sustain the normal physiological function of cells.<sup>21,22</sup> However, prolonged exposure to CCl<sub>4</sub> inevitably increased oxidative stress damage and led to the consequent unfolded protein response (UPR), disrupting the function of the endoplasmic reticulum. Under this condition, ERS response gradually switches from pro-survival to pro-apoptosis.<sup>23</sup> ERS can be implicated in a variety of diseases; especially, it has been considered as a major contributor to hepatic fibrosis.<sup>24</sup> The present study showed that CCl<sub>4</sub> triggered intense ERS by promoting the expression of GRP78, XBP1 and ATF6, as well as the PERK/eIF2 $\alpha$  and IRE1 $\alpha$  paths. Meanwhile, the ERS-mediated apoptotic proteins (CHOP and p-JNK/JNK) were also markedly increased, suggesting that CCl<sub>4</sub>-induced excessive ERS led to hepatocyte apoptosis. However, didymin or 4PBA significantly reversed the abnormal changes induced by CCl<sub>4</sub>. These findings demonstrated that didymin could reduce ERS, which contributed to suppressing liver fibrogenesis.

The prediction of transcriptomics analysis showed oxidative stress and inflammation might also be involved in the regulation of didymin on fibrogenesis. When tissue is exposed to CCl<sub>4</sub>, ROS production will outweigh the antioxidant defense system's ability to degrade ROS, and then oxidative stress occurs, resulting in ROS accumulation.<sup>25</sup> Usually, to achieve rebalance in the oxidation levels, cells in the liver either down-regulate the production of ROS or activate antioxidant systems. Meanwhile, oxidative stress and inflammation are reciprocal causes and outcomes. With the decreased oxidation levels, iNOS was reduced; subsequently, the same trend was observed in nitric oxide (NO), an important inflammatory mediator. In the current study, didymin administration significantly decreased the production of ROS and enhanced the expressions of antioxidant enzymes such as CAT, GSH and SOD. Besides, pro-inflammatory cytokines, IL1 $\beta$  and IL6, were also significantly inhibited by didymin. The results suggested that didymin might attenuate liver fibrosis by mitigating CCl<sub>4</sub>-induced oxidative stress and inflammatory response.

Previous experiment results suggest that pathological apoptosis of hepatocytes is closely related to the occurrence of hepatic fibrosis.<sup>26</sup> As shown in the TUNEL staining, mice treated with CCl<sub>4</sub> showed severe apoptosis, with many apoptosis cells densely distributed in the interlobular septa. In contrast, didymin administration greatly decreased the number of apoptosis cells, alleviating hepatic apoptosis. To expose the potential mechanism, we further investigated the relationship between hepatocyte apoptosis and mitochondrial dysfunction. After CCl<sub>4</sub> modeling, plenty of superoxide radicals were generated and damaged mitochondria, resulting in cytochrome C releasing from mitochondria into the cytosol and triggering cytochrome c/caspase-9 signaling, a mitochondrial-dependent intrinsic apoptosis pathway.<sup>27</sup> Meanwhile, the mitochondrial apoptotic pathway is regulated by the Bcl-2 family. In the present study, didymin significantly reduced the expression of Bax and enhanced the Bcl-2 level, rebuilding the balance of Bax/Bcl-2. Besides, didymin significantly reduced the release of cytochrome c and decreased the Caspase-9 cascade reaction, suggesting didymin could maintain mitochondrial membrane integrity. These results indicated that the protective effects of didymin against hepatic fibrosis were attributed to its ability to alleviate hepatic apoptosis and preserve mitochondrial function, to some extent.

Metabolic disturbance may lead to various dysfunction, including liver injury. According to the prediction of transcriptomic analysis, we also focused on whether the protective effect of didymin on liver injury and fibrosis was associated with metabolism. We found that there were different 454 metabolites in the liver lysates between the didymin and CCl<sub>4</sub> groups (269 up- and 185 down-regulated metabolites), which were mainly enriched in the glycerophospholipid metabolism pathway (P-value < 0.05). It is well known that glycerophospholipids are the essential component of cellular membranes and a source of physiologically active compounds, which serve as signaling molecules and as anchors for proteins in cell membranes.<sup>28</sup> Excessive glycerophospholipids in hepatocytes may cause lipid toxicity, ultimately destroying hepatocytes. In this study, the integrated analyses of metabolomics and transcriptomics indicated that didymin inhibited the glycerophospholipid metabolism pathway by reducing the synthesis of the target metabolites (phosphatidylethanolamines and phosphatidylcholines) via regulating the target genes expression (LPCAT1, LPCAT3, LPIN1, PCYT1 $\alpha$ , PCYT2, and DGKZ). These data suggested that didymin could restore glycerophospholipid metabolism, which was beneficial to alleviate hepatocyte damage and fibrosis.

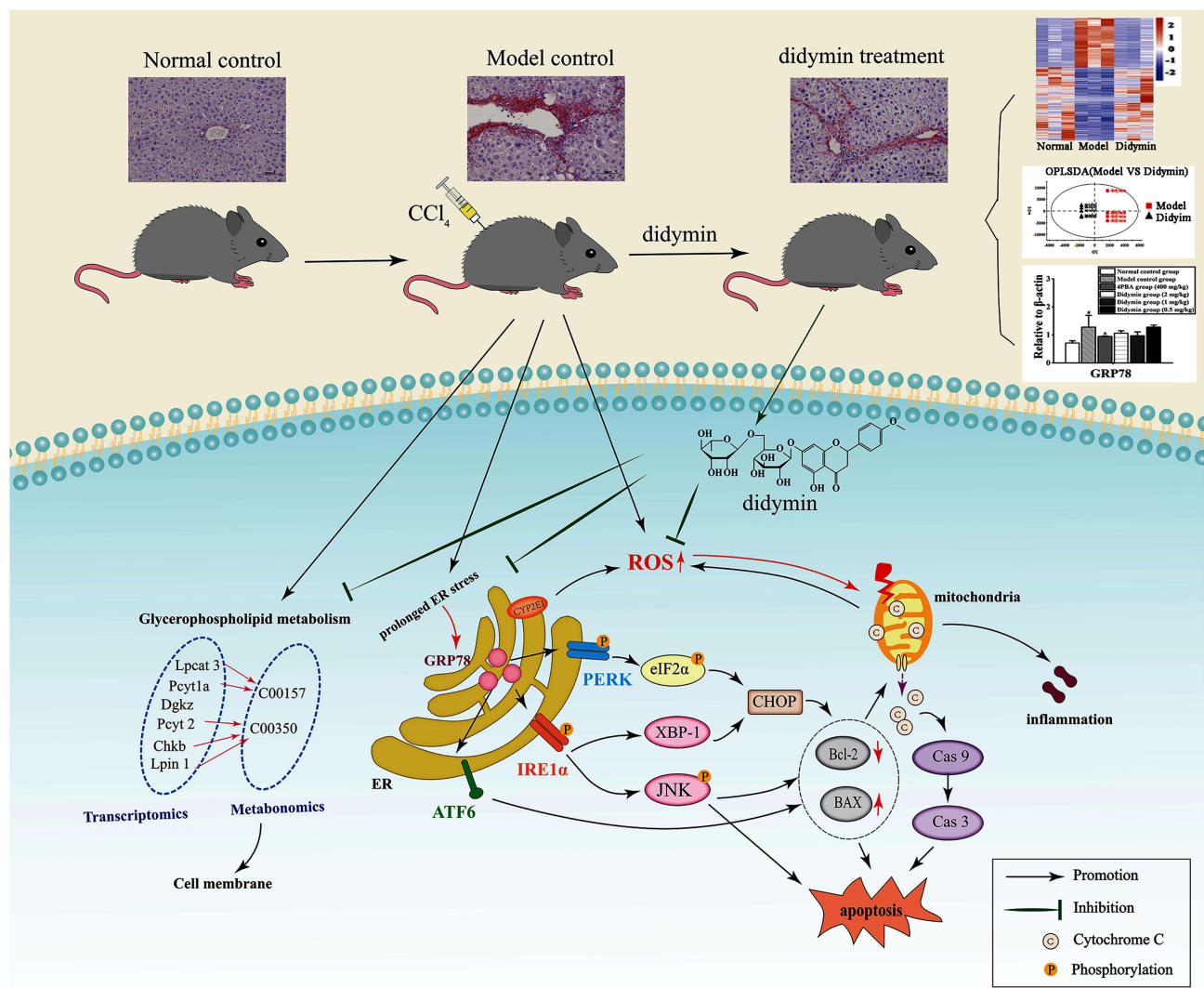


**Figure 12** Didymmin ameliorates liver fibrosis by reducing ERS, hepatic apoptosis, and inflammation, as well as mediating glycerophospholipid metabolism.

## Conclusions

In conclusion, didymmin shows significant effects in alleviating hepatic fibrosis, which is mainly attributed to the inhibition of ERS, apoptosis, inflammation, and glycerophospholipid metabolism as well (Figure 12). Didymmin may be developed as a promising agent for the treatment of hepatic fibrosis.

## Data Sharing Statement

The transcriptomics data (RNA-sequencing) can be found in <https://www.ncbi.nlm.nih.gov/geo/query/acc.cgi?acc=GSE189409>; the metabolomics data is published at [www.ebi.ac.uk/metabolights/MTBLS3889](http://www.ebi.ac.uk/metabolights/MTBLS3889); the raw data can be found in the [Supplementary Materials](#).

## Acknowledgments

The authors gratefully acknowledge the financial support provided by the National Natural Science Foundation of China (No. 81873087), the Guangxi Natural Science Foundation (2018GXNSFDA281048), and the National Natural Science Foundation of China (No. 82060755).

## Disclosure

The authors declare that they have no conflicts of interest for this work nor regarding the publication of this paper.

## References

1. Du XS, Li HD, Yang XJ, et al. Wogonin attenuates liver fibrosis via regulating hepatic stellate cell activation and apoptosis. *Int Immunopharmacol.* 2019;75:105671. doi:10.1016/j.intimp.2019.05.056
2. Wang XM, Peng PK, Pan ZQ, et al. Psoralen inhibits malignant proliferation and induces apoptosis through triggering endoplasmic reticulum stress in human SMMC7721 hepatoma cells. *Biol Res.* 2019;52(1):34. doi:10.1186/s40659-019-0241-8
3. Yu X, Wang T, Zhu M, et al. Transcriptome and physiological analyses for revealing genes involved in wheat response to endoplasmic reticulum stress. *BMC Plant Biol.* 2019;19(1):193. doi:10.1186/s12870-019-1798-7
4. Jia J, Qin J, Yuan X, et al. Microarray and metabolome analysis of hepatic response to fasting and subsequent refeeding in zebrafish (*Danio rerio*). *BMC Genom.* 2019;20(1):919. doi:10.1186/s12864-019-6309-6
5. Han CY, Rho HS, Kim A, et al. FXR inhibits endoplasmic reticulum stress-induced NLRP3 inflammasome in hepatocytes and ameliorates liver injury. *Cell Rep.* 2018;24(11):2985–2999. doi:10.1016/j.celrep.2018.07.068
6. Li XH, Wang YR, Wang H, et al. Endoplasmic reticulum stress is the crossroads of autophagy, inflammation, and apoptosis signaling pathways and participates in liver fibrosis. *Inflam Res.* 2015;64(1):1–7. doi:10.1007/s00011-014-0772-y
7. Zambo V, Simon-Szabo L, Szelenyi P, et al. Lipotoxicity in the liver. *World J Hepatol.* 2013;5(10):550–557. doi:10.4254/wjh.v5.i10.550
8. Buechler C, Aslanidis C. Role of lipids in pathophysiology, diagnosis and therapy of hepatocellular carcinoma. *Biochim Biophys Acta Mol Cell Biol Lipids.* 2020;1865(5):158658. doi:10.1016/j.bbalip.2020.158658
9. Wang S, Tang K, Lu Y, et al. Revealing the role of glycerophospholipid metabolism in asthma through plasma lipidomics. *Clin Chim Acta.* 2021;513:34–42. doi:10.1016/j.cca.2020.11.026
10. Zhou Y, Wu R, Cai FF, et al. Xiaoyaosan decoction alleviated rat liver fibrosis via the TGFβ/Smad and Akt/FoxO3 signaling pathways based on network pharmacology and transcriptomic analysis. *J Ethnopharmacol.* 2020;264:113021. doi:10.1016/j.jep.2020.113021
11. Sikander M, Malik S, Parveen K, et al. Hepatoprotective effect of *Origanum vulgare* in Wistar rats against carbon tetrachloride-induced hepatotoxicity. *Protoplasm.* 2013;250(2):483–493. doi:10.1007/s00709-012-0431-5
12. Feng Z, Pang L, Chen S, et al. Didymin ameliorates dexamethasone-induced non-alcoholic fatty liver disease by inhibiting TLR4/NF-κB and PI3K/Akt pathways in C57BL/6J mice. *Int Immunopharmacol.* 2020;88:107003. doi:10.1016/j.intimp.2020.107003
13. Huckins LM, Chatzinakos C, Breen MS, et al. Analysis of genetically regulated gene expression identifies a prefrontal PTSD gene, SNRNP35, specific to military cohorts. *Cell Rep.* 2020;31(9):107716. doi:10.1016/j.celrep.2020.107716
14. Wu Y, Li Z, Xiu AY, et al. Carvedilol attenuates carbon tetrachloride-induced liver fibrosis and hepatic sinusoidal capillarization in mice. *Drug Des Devel Ther.* 2019;13:2667–2676. doi:10.2147/DDDT.S210797
15. Du K, Hyun J, Premont RT, et al. Hedgehog-YAP signaling pathway regulates glutaminolysis to control activation of hepatic stellate cells. *Gastroenterology.* 2018;154(5):1465–1479 e1413. doi:10.1053/j.gastro.2017.12.022
16. Li F, Liu G, Xue P, et al. YiQi YangYin decoction attenuates nonalcoholic fatty liver disease in type 2 diabetes rats. *Evid Based Complement Alternat Med.* 2021;2021:5511019. doi:10.1155/2021/5511019
17. Yu SH, Zhu KY, Chen J, et al. JMJD3 facilitates C/EBPβ-centered transcriptional program to exert oncorepressor activity in AML. *Nat Commun.* 2018;9(1):3369. doi:10.1038/s41467-018-05548-z
18. Zhou Q, Song N, Wang SQ, et al. Effect of gegen qinlian decoction on hepatic gluconeogenesis in ZDF rats with type 2 diabetes mellitus based on the farnesol X receptor/ceramide signaling pathway regulating mitochondrial metabolism and endoplasmic reticulum stress. *Evid Based Complement Alternat Med.* 2021;2021:9922292. doi:10.1155/2021/9922292
19. Ferrarini A, Di Poto C, He S, et al. Metabolomic analysis of liver tissues for characterization of hepatocellular carcinoma. *J Proteome Res.* 2019;18(8):3067–3076. doi:10.1021/acs.jproteome.9b00185
20. Sharma A, Anand SK, Singh N, et al. Berbamine induced activation of the SIRT1/LKB1/AMPK signaling axis attenuates the development of hepatic steatosis in high-fat diet-induced NAFLD rats. *Food Funct.* 2021;12(2):892–909. doi:10.1039/d0fo02501a
21. Roe ND, Ren J. Oxidative activation of Ca<sup>2+</sup>/calmodulin-activated kinase II mediates ER stress-induced cardiac dysfunction and apoptosis. *Am J Physiol Heart Circul Physiol.* 2013;304(6):H828–H839. doi:10.1152/ajpheart.00752.2012
22. Long P, He M, Yan W, et al. ALDH2 protects naturally aged mouse retina via inhibiting oxidative stress-related apoptosis and enhancing unfolded protein response in endoplasmic reticulum. *Aging.* 2020;13(2):2750–2767. doi:10.18632/aging.202325
23. Yun W, Yu-Han G, Ming L, et al. TBHQ alleviated endoplasmic reticulum stress-apoptosis and oxidative stress by PERK-Nrf2 crosstalk in methamphetamine-induced chronic pulmonary toxicity. *Oxid Med Cell Longev.* 2017;2017:4310475. doi:10.1155/2017/4310475
24. Koo JH, Lee HJ, Kim W, Kim SG. Endoplasmic reticulum stress in hepatic stellate cells promotes liver fibrosis via PERK-mediated degradation of HNRNPA1 and up-regulation of SMAD2. *Gastroenterology.* 2016;150(1):181–193 e188. doi:10.1053/j.gastro.2015.09.039
25. Xu J, Zhang G, Tong Y, et al. Corilagin induces apoptosis, autophagy and ROS generation in gastric cancer cells in vitro. *Int J Mol Med.* 2019;43(2):967–979. doi:10.3892/ijmm.2018.4031
26. Wang R, Song F, Li S, et al. Salvianolic acid A attenuates CCl<sub>4</sub>-induced liver fibrosis by regulating the PI3K/AKT/mTOR, Bcl-2/Bax and caspase-3/cleaved caspase-3 signaling pathways. *Drug Des Devel Ther.* 2019;13:1889–1900. doi:10.2147/DDDT.S194787
27. Liu YM, Cong S, Cheng Z, et al. Platycodin D alleviates liver fibrosis and activation of hepatic stellate cells by regulating JNK/c-JUN signal pathway. *Eur J Pharmacol.* 2020;876:172946. doi:10.1016/j.ejphar.2020.172946
28. Kartsoli S, Kostara CE, Tsimihodimos V, et al. Lipidomics in non-alcoholic fatty liver disease. *World J Hepatol.* 2020;12(8):436–450. doi:10.4254/wjh.v12.i8.436



Drug Design, Development and Therapy

Dovepress

### Publish your work in this journal

Drug Design, Development and Therapy is an international, peer-reviewed open-access journal that spans the spectrum of drug design and development through to clinical applications. Clinical outcomes, patient safety, and programs for the development and effective, safe, and sustained use of medicines are a feature of the journal, which has also been accepted for indexing on PubMed Central. The manuscript management system is completely online and includes a very quick and fair peer-review system, which is all easy to use. Visit <http://www.dovepress.com/testimonials.php> to read real quotes from published authors.

Submit your manuscript here: <https://www.dovepress.com/drug-design-development-and-therapy-journal>